
Adaptive Learning Rates with Maximum Variation Averaging

Chen Zhu¹, Yu Cheng², Zhe Gan², Furong Huang¹, Jingjing Liu², Tom Goldstein¹

¹University of Maryland, College Park, ²Microsoft Dynamics 365 AI Research
{chenzhu, furongh, tomg}@cs.umd.edu
{yu.cheng, zhe.gan, jingjl}@microsoft.com

Abstract

Adaptive gradient methods such as RMSPROP and ADAM use exponential moving estimate of the squared gradient to compute element-wise adaptive step sizes and handle noisy gradients. However, ADAM can have undesirable convergence behavior in some problems due to unstable or extreme adaptive learning rates. Methods such as AMSGRAD and ADABOUND have been proposed to stabilize the adaptive learning rates of ADAM in the later stage of training, but they do not outperform ADAM in some practical tasks such as training Transformers [26]. In this paper, we propose an adaptive learning rate rule in which the running mean squared gradient is replaced by a weighted mean, with weights chosen to maximize the estimated variance of each coordinate. This gives a worst-case estimate for the local gradient variance, taking smaller steps when large curvatures or noisy gradients are present, resulting in more desirable convergence behavior than ADAM. We analyze and demonstrate the improved efficacy of our adaptive averaging approach on image classification, neural machine translation and natural language understanding tasks.¹

1 Introduction

SGD and its variants are both efficient and effective in training deep neural networks despite their simplicity. In their simplest form, gradient methods train a network by iteratively moving each parameter in the direction of the negative gradient (or the running average of gradients) of the loss function on a randomly sampled mini-batch of training data, as well as a scalar learning rate to control the size of the update. In contrast, *adaptive* stochastic methods use coordinate-specific learning rates inversely proportional to the square root of a running mean of squared gradients [25, 6, 11]. Such methods have been proposed to improve the stability of SGD on non-stationary problems, and have achieved success in training models for various fields including Speech, Computer Vision (CV), and Natural Language Processing (NLP).

Despite the popularity of adaptive methods such as Adam [11], the instability of adaptive learning rates sometimes results in worse generalization performance than traditional SGD, converging to sub-optimal solutions on some simple problems, or even exhibiting non-convergent behavior [28, 21, 16]. AMSGRAD [21] was proposed to stabilize ADAM by computing the adaptive learning rate with an update rule that guarantees monotonically decaying adaptive learning rates for each coordinate. ADABOUND [16] clips the adaptive learning rate of ADAM with a decreasing upper bound and an increasing lower bound, so that it converges to SGD in the final stage of training. However, to our knowledge, neither of the two approaches have been deployed to enhance ADAM on recent large-scale problems such as training Transformer-based language models [5, 14, 12, 20, 36]. The stochastic gradients of Transformer’s loss functions exhibit heavy-tailed statistics, making SGD

¹Our code is available at <https://github.com/zhuchen03/mva>.

unstable unless training begins with a small “warmup” learning rate. And [34] has to use clipping to stabilize SGD for training transformers, indicating that the strategy of ADABOUND might fail on Transformers since it transitions to SGD. RAdam [13] was recently invented to free ADAM from the warmup schedule for training Transformers, but its variance rectification term does not really depend on the observed gradients during training, and [17] found that using a linear warmup over $2 \cdot (1 - \beta_2)^{-1}$ iterations for ADAM achieves almost the same convergence as RAdam.

In this work, we explore a different approach to improve the stability of adaptive learning rates. We propose *Maximum Variation Averaging* (MVA), which computes the running average of squared gradients using dynamic, rather than constant, coordinate-wise weights. These weights are chosen so that the estimated variance of gradients is maximized. The MVA weights for maximizing this variance have a simple closed-form solution that requires little storage or computational cost, yet is able to improve the test set performance of ADAM on a variety of CV and NLP tasks.

2 Background & Definitions

We introduce some preliminary definitions before diving into the proposed method. By default, all vector-vector operators will be element-wise in the following sections. Let $\theta \in \mathbb{R}^d$ be the parameters of the network to be trained, $\ell(x; \theta)$ is the loss of the model with parameters θ evaluated at x . Our goal is to minimize the expected risk on the data distribution defined as:

$$\mathcal{L}(\theta) = \mathbb{E}_{x \sim \mathcal{D}} [\ell(x; \theta)]. \quad (1)$$

In most deep learning problems, only a finite number of potentially noisy samples can be used to approximate Eq. 1, and the gradients are computed on randomly sampled minibatches during training. Stochastic regularizations like Dropout [24] further adds to the randomness of the gradients, and are commonly used with Transformers [26]. Thus, it is important to design optimizers that tolerate noisy gradients.

ADAM [11] is an effective optimizer that adapts to such noisy gradients. It keeps exponential averages of the gradient and its square, m_t and v_t , defined as:

$$\begin{aligned} \tilde{m}_t &= \alpha \tilde{m}_{t-1} + (1 - \alpha) g_t, & m_t &= \frac{\tilde{m}_t}{1 - \alpha^{t+1}}, \\ \tilde{v}_t &= \beta \tilde{v}_{t-1} + (1 - \beta) g_t^2, & v_t &= \frac{\tilde{v}_t}{1 - \beta^{t+1}}, \end{aligned} \quad (2)$$

where $\alpha, \beta \in [0, 1]$, and $\tilde{m}_0 = \tilde{v}_0 = 0$, and parameters are updated by:

$$\theta_{t+1} = \theta_t - \eta_t \frac{m_t}{\sqrt{v_t} + \epsilon}, \quad (3)$$

where $\epsilon > 0$ is typically a small constant for numerical stability. If we assume that the distribution of the stochastic gradient is constant within the effective horizon of the running average [1], an assumption that is more accurate when the model is closer to convergence, then m_t and v_t will be estimates of the first and second moment of the gradient g_t . Specifically, we analyze adaptive learning rates through the lens of the following assumption:

Assumption 1 Let σ_t^2 be the variance of g_t . At time t , assume $\mathbb{E}[m_t] \approx \nabla \mathcal{L}_t$, $\mathbb{E}[v_t] \approx \nabla \mathcal{L}_t^2 + \sigma_t^2$.

Under this assumption, the update step $m_t / \sqrt{v_t}$ of ADAM can be seen as an approximation to the Signal-to-Noise Ratio (SNR) of the gradient, which results in smaller steps when the SNR is low [11]. RMSPROP [25] and other variants that divide the update steps by $\sqrt{v_t}$ can also be seen as adapting to the gradient variance under the same assumption [1]. These adaptive methods take smaller step sizes when the estimated variance $\tilde{\sigma}_t^2 = v_t - m_t^2$ is high. Higher local gradient variance indicates higher local curvature, and in certain quadratic approximations to the loss function, this variance is directly proportional to the curvature [22] (Eq. 13 of our paper). Therefore, similar to a diagonal approximation to Newton’s method, using smaller learning rates in these directions can improve convergence of first-order methods.

However, the adaptive learning rate $\eta_t / (\sqrt{v_t} + \epsilon)$ of ADAM and RMSPROP can take extreme values, making it unable to converge to the desired solution of some simple problems [28, 4]. [21] gave one of such counter examples where gradients in the correct direction are large but occur at a low frequency, and ADAM converges to the solution with a maximum regret. They solve this issue by

keeping track of the maximum v_t for each coordinate throughout training with a new variable \hat{v}_t , and change the adaptive learning rate into $\eta_t/\sqrt{\hat{v}_t}$ to enforce monotonically decreasing learning rates. Extremely small adaptive learning rates can also cause undesirable convergence behavior, as demonstrated by a counter example in [16].

3 Maximizing the Variance of Running Estimations

Algorithm 1 MADAM

1: **Input:** Learning rate $\{\eta_t\}_{t=1}^T$, parameter $0 < \alpha < 1, 0 < \beta < \tilde{\beta} < 1, \epsilon > 0$
2: Set $\tilde{m}_0 = \tilde{u}_0 = \tilde{v}_0 = w_0 = 0$
3: **for** $t = 1$ **to** T **do**
4: Draw samples S_t from training set
5: Compute $g_t = \frac{1}{|S_t|} \sum_{x_k \in S_t} \nabla \ell(x_k; \theta_t)$
6: $\tilde{m}_t = \alpha \tilde{m}_{t-1} + (1 - \alpha) g_t$
7: $\tilde{\beta}_t = \arg \max_{\beta} v_t(\beta) - u_t^2(\beta)$ ▷ see Eq 8
8: $\beta_t = \max(\beta, \min(\tilde{\beta}, \tilde{\beta}_t))$
9: $\tilde{u}_t = \beta_t \tilde{u}_{t-1} + (1 - \beta_t) g_t$
10: $\tilde{v}_t = \beta_t \tilde{v}_{t-1} + (1 - \beta_t) g_t^2$
11: $w_t = \beta_t w_{t-1} + (1 - \beta_t)$
12: $\theta_t = \theta_{t-1} - \eta_t \frac{\sqrt{w_t}}{1 - \alpha^t} \frac{\tilde{m}_t}{\sqrt{\tilde{v}_t + \epsilon}}$

Algorithm 2 LAMADAM

1: **Input:** Learning rate $\{\eta_t\}_{t=1}^T$, parameter $0 < \alpha < 1, 0 < \beta < \tilde{\beta} < 1, \epsilon > 0$
2: Set $\tilde{m}_0 = \tilde{u}_0 = \tilde{v}_0 = w_0 = 0$
3: **for** $t = 1$ **to** T **do**
4: Draw samples S_t from training set
5: Compute $g_t = \frac{1}{|S_t|} \sum_{x_k \in S_t} \nabla \ell(x_k; \theta_t)$
6: $\tilde{\beta}_t = \arg \max_{\beta} v_t(\beta) - u_t^2(\beta)$ ▷ see Eq 8
7: $\beta_t = \max(\beta, \min(\tilde{\beta}, \tilde{\beta}_t))$
8: $\tilde{u}_t = \beta_t \tilde{u}_{t-1} + (1 - \beta_t) g_t$
9: $\tilde{v}_t = \beta_t \tilde{v}_{t-1} + (1 - \beta_t) g_t^2$
10: $w_t = \beta_t w_{t-1} + (1 - \beta_t)$
11: $\tilde{m}_t = \alpha \tilde{m}_{t-1} + (1 - \alpha) \frac{g_t}{\sqrt{\tilde{v}_t/w_t + \epsilon}}$
12: $\theta_t = \theta_{t-1} - \frac{\eta_t}{1 - \alpha^t} \tilde{m}_t$

Motivation. We propose to mitigate the undesirable convergence issue of ADAM by changing the constant running average coefficient β for the second moment into an adaptive one. The idea is to allow β_t to adopt the value that maximizes the estimated covariance of the gradient at each iteration t . Therefore, our algorithm can use β_t as the adaptive running average coefficient to take steps that are conservative enough to avoid instability but aggressive enough to make progress.

Maximum Variation Averaging. Formally, we estimate the variance of the gradient at each coordinate by keeping track of the zeroth, first, and second moment of the gradient as functions of the adaptive running average coefficient β_t , denoted as $w_t(\beta_t)$, $\tilde{u}_t(\beta_t)$ and $\tilde{v}_t(\beta_t)$, respectively:

$$w_t(\beta_t) = \beta_t w_{t-1}(\beta_{t-1}) + (1 - \beta_t), \quad (4)$$

$$\tilde{u}_t(\beta_t) = \beta_t \tilde{u}_{t-1}(\beta_{t-1}) + (1 - \beta_t) g_t, \quad (5)$$

$$\tilde{v}_t(\beta_t) = \beta_t \tilde{v}_{t-1}(\beta_{t-1}) + (1 - \beta_t) g_t^2. \quad (6)$$

The zeroth moment $w_t(\beta_t)$ tracks the total weight used for averaging, and is used to normalize $\tilde{u}_t(\beta_t)$ and $\tilde{v}_t(\beta_t)$ to achieve unbiased estimates $u_t(\beta_t) = \tilde{u}_t(\beta_t)/w_t(\beta_t)$ and $v_t(\beta_t) = \tilde{v}_t(\beta_t)/w_t(\beta_t)$ for the first and second moment [11].

Then, the unbiased local estimate of the gradient variance is $\tilde{\sigma}_t^2 = \tilde{v}_t(\beta_t)/w_t(\beta_t) - [\tilde{u}_t(\beta_t)/w_t(\beta_t)]^2$. Through an argmax optimization, we find the β_t that achieves the worst-case (maximal) variance for each coordinate

$$\beta_t = \arg \max_{\beta} \tilde{\sigma}_t^2 = \arg \max_{\beta} v_t(\beta) - [u_t(\beta)]^2. \quad (7)$$

We call our approach for finding adaptive running average coefficient β_t *Maximum Variation Averaging* (MVA). We plug MVA into ADAM and its variant, LAPROP [37], which results in two novel algorithms, MADAM and LAMADAM, listed in Algorithm 1 and Algorithm 2. LAPROP uses local running estimation of the variance to normalize the gradients before taking the running average, which results in higher empirical stability under various hyperparameters. Note, we only use the MVA formula for the *second* moment $u_t(\beta_t)$ used for scaling the learning rate; m_t is still an exponential moving average (with a constant coefficient α) for the gradient of MADAM or the normalized gradient of LAMADAM.

Finding β_t via a closed-form solution. The maximization for β_t in Eq. 7 is quadratic and has a relatively simple closed-form solution that produces maximal $\tilde{\sigma}_t^2$ for each coordinate. This is given by

$$\beta_t = \frac{(g_t - u_{t-1})^2 + v_{t-1} - u_{t-1}^2}{w_{t-1}((g_t - u_{t-1})^2 - v_{t-1} + u_{t-1}^2) + (g_t - u_{t-1})^2 + v_{t-1} - u_{t-1}^2}, \quad (8)$$

where we have abbreviated $u_{t-1}(\beta_{t-1})$, $v_{t-1}(\beta_{t-1})$ and $w_{t-1}(\beta_{t-1})$ into \tilde{u}_{t-1} , \tilde{v}_{t-1} and w_{t-1} , and will use this abbreviation by default in the following sections. We defer the derivation of Eq. 8 to Appendix A.

Practical notes. We apply MVA in every step except for the first step, where the gradient variance we can observe is 0. The coefficient for $t = 1$ is set to a constant β_1 that is the same as typical values for ADAM, and for Algorithm 1 and Algorithm 2 we define

$$\tilde{u}_1 = (1 - \beta_1)g_1, \tilde{v}_1 = (1 - \beta_1)g_1^2, w_1 = 1 - \beta_1. \quad (9)$$

To obtain a valid running average, we clip β_t so that $\underline{\beta} \leq \beta_t \leq \bar{\beta}$, where the typical values are $\underline{\beta} = 0.5, 0.98 \leq \bar{\beta} \leq 1$. For convenience, we set $\beta_1 = \bar{\beta}$ by default. For $t > 1$, since $0 < \beta_t \leq 1$, w_t will monotonically increase from $(1 - \beta_1)$ to 1. Before clipping, for any g_t, u_{t-1}, v_{t-1} satisfying $v_{t-1} - u_{t-1}^2 > 0$ in Eq. 8, we have $\beta_t \in [1/(1 + w_{t-1}), 1/(1 - w_{t-1})]$. As a result, the lower bound that we use ($\underline{\beta} = 0.5$) is tight and does not really change the value of β_t , and as $t \rightarrow \infty, w_t \rightarrow 1$ and $\beta_t \in [0.5, \infty]$. We have a special case at $t = 2$, where β_t is a constant $1/(2 - \beta_1)$.

In practice, we also add a small coefficient $\delta > 0$ to the denominator of Eq. 8 to prevent division by zero, which will have negligible effect on the value of β_t and does not violate the maximum variation objective (Eq. 7). All the derivations for these conclusions are deferred to Appendix B.

The effect of Maximum Variation Averaging. In most cases, $v_{t-1} - u_{t-1}^2 > 0$. If we define a new variable $R_t = (g_t - u_{t-1})^2 / (v_{t-1} - u_{t-1}^2)$, which represents the degree of deviation of gradient g_t from the current estimated average, we can rewrite

$$\beta_t = \frac{R_t + 1}{(1 + w_t)R_t + 1 - w_t}. \quad (10)$$

From Eq. 10, we can see β_t monotonically decreases from $1/(1 - w_t)$ to $1/(1 + w_t)$ as R_t increases from 0 to ∞ , and equals to 1 when $R_t = 1$. As a result, for each entry, if $R_t \leq 1$, or the deviation of the gradient g_t from the current running mean \tilde{u}_{t-1} is within the estimated standard deviation $\tilde{\sigma}$, we will use $\bar{\beta}$ to update \tilde{v}_t , which is the slowest change we allow for \tilde{v}_t . If g_t deviates much more than $\tilde{\sigma}$, MVA will find a smaller β_t and therefore a higher weight $(1 - \beta_t)$ on g_t^2 to adapt to the change faster. This allows a quick response to impede abnormally large gradients, which enables a better handling for the heavy-tailed distribution of gradients in the process of training Transformers [34]. As a side effect, \tilde{v}_t tends to be larger than ADAM/LAPROP using a constant $\bar{\beta}$, but as we will show in the experiments, using a larger learning rate counters such an effect and achieves better results.

On the other hand, when the variance decreases in the later phase of training, g_t tends to be within $\tilde{\sigma}_t$, and MVA tends to find the slowest rate for decreasing \tilde{v}_t . This allows large values of \tilde{v}_t to last for a longer horizon even compared with setting β_t to a constant $\bar{\beta}$ on the same sequence, since we have assigned more mass to large gradients, which can be seen as an adaptive version of AMSGRAD.

4 Analysis with Simulations

4.1 Convergence with Stochastic Gradients

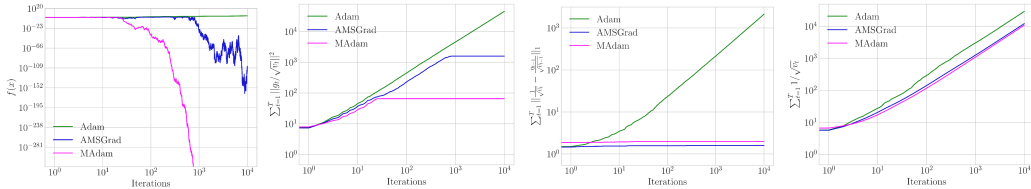


Figure 1: Objective value, Term A, Term B and $s_2(T)$ [4] of ADAM, AMSGRAD, MADAM on the problem defined in Eq. 11. The constant learning rate is cancelled here since we only care about the ratios.

We will analyze the convergence of MADAM through an illustrative example from [4] which simulates the process of stochastic gradient descent. Theoretical results are left as future work, but we evaluate the terms of the convergence rate obtained in Theorem 3.1 of [4] and shed some lights on the theoretical analysis. Formally, we consider the problem $\min_{\theta} \mathcal{L}(\theta) = \sum_{i=1}^{11} \ell_i(\theta)$ where

$$\ell_i(\theta) = \begin{cases} \mathbb{I}[i = 1]5.5\theta^2 + \mathbb{I}[i \neq 1](-0.5\theta^2), & \text{if } |\theta| \leq 1; \\ \mathbb{I}[i = 1](11|\theta| - 5.5) + \mathbb{I}[i \neq 1](-|\theta| + 0.5), & \text{otherwise.} \end{cases} \quad (11)$$

At every step, a random index i is sampled uniformly from $i \in [11]$, and the randomness of this problem only comes from stochastic sampling. The only stationary point where $\nabla \mathcal{L} = 0$ is $\theta = 0$. We compare ADAM, AMSGRAD and MADAM on optimizing this objective, where we use constant learning rates η in every step, and set $\alpha = 0, \beta = 0.9$ for ADAM and AMSGRAD, and $\alpha = 0, (\underline{\beta}, \bar{\beta}) = (0.5, 1)$ for MADAM. ADAM never converged for a variety of η we tried within $[10^{-4}, 1]$, consistent with [4]. Generally, a larger η gives faster convergence for both AMSGRAD and MADAM. For reproducibility, we repeat experiments 100 times with the same settings, and choose the η for AMSGRAD and MADAM where the solution $|\theta^*| < 0.1$ every time. $\eta = 1.2$ satisfies this requirement for MADAM, but AMSGRAD only satisfied it 1% of the times for $\eta = 1.2$ and 65% of the times for $\eta = 0.9$. $\eta = 0.8$ is the largest η we find for AMSGRAD to achieve 100% satisfaction. Therefore, we use $\eta = 0.8$ for both ADAM and AMSGRAD.

We plot the values of the objective, Term A, Term B and $s_2(T)$ of Theorem 3.1 of [4] in Figure 4.1. We can conclude from the objective value that MADAM fixes up the divergence issue of ADAM, and converges faster than AMSGRAD on this problem. This result is also consistent with Theorem 3.1 of [4] from the observation that MADAM has a significant smaller Term A, a Term B that is only slightly larger than AMSGRAD, and a $s_2(T)$ that is only slightly smaller than AMSGRAD. How to condense these terms with the hyperparameters from MVA to prove an improved convergence rate is an interesting future direction.

4.2 Convergence in the Noisy Quadratic Model

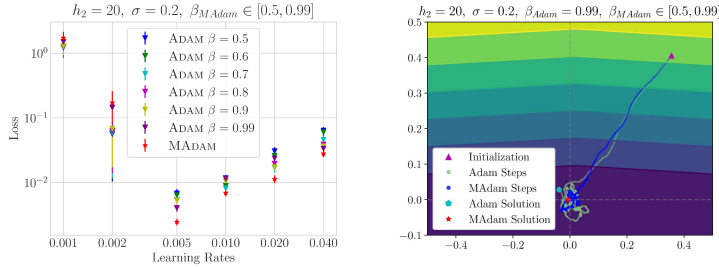


Figure 2: Results on the noisy quadratic model. The left figure shows the average loss and its standard error under different learning rates. Figure on the right gives a qualitative example of the trajectories of two approaches. The best solution of MADAM is better than ADAM under all β evaluated. Comparing the best solutions of two methods, MADAM achieves both lower average loss and lower standard error at convergence ($2.46\text{e-}3$ ($2.94\text{e-}4$) vs. $4.05\text{e-}3$ ($4.82\text{e-}4$) at learning rate 0.005).

We analyze the ability of MADAM to adapt to curvature and noise on the simple but illustrative “noisy quadratic model”, which has been widely adopted for analyzing the optimization dynamics [22, 29, 33, 35]. The loss function is defined as:

$$\mathcal{L}(\theta) = \mathbb{E}_{x \sim \mathcal{N}(0, \sigma^2 I)} \left[\frac{1}{2} \sum_{i=1}^d h_i (\theta_i - x_i)^2 \right], \quad (12)$$

where x is a noisy observation of the ground-truth parameter $\theta^* = 0$, simulating the gradient noise in stochastic optimization, and h_i represents the curvature of the system in d dimensions. In each step, the algorithm takes the following noisy gradient for dimension i as the input:

$$\nabla_{\theta_i} \tilde{\mathcal{L}}(\theta) = h_i (\theta_i - \sigma \epsilon_i), \epsilon_i \sim \mathcal{N}(0, 1), \quad (13)$$

from which we can see the gradient noise is proportional to the curvature h_i .

To verify the effectiveness of MVA, we compare MADAM with ADAM under a variety of different curvature h and noise level σ on a 2D problem ($d = 2$). For each instance of the problem, we test both algorithms on a variety of learning rates. We set $\underline{\beta} = 0.5, \bar{\beta} = 0.99$ for MADAM, and for fair comparison, we test ADAM with $\beta = 0.5, 0.6, 0.7, 0.8, 0.9, 0.99$. We repeat the experiments 100 times under each setting, where we select a random initialization of $\theta \sim \mathcal{N}(0, I)$ each time, and run MADAM and ADAM with different hyper-parameters from this random initialization. We take the mean and standard error of the 100 runs for comparison, where MADAM consistently achieves 30% to 40% lower average loss with smaller standard error. Figure 2 shows the results for one of the instances, from which we find the best results of MADAM is consistently better than ADAM under

all choices of β , confirming the difference MVA has made by choosing an adaptive β_t . From the qualitative example, MVA also demonstrates smaller variance near convergence, caused by a more aggressive response to impede the noise with a smaller β_t . We provide more experimental results under other settings in Appendix C.

5 Experiments with Practical Datasets

In this section, we thoroughly evaluate MADAM and LAMADAM on a variety of tasks against well-calibrated baselines: CIFAR10/100 and ImageNet for image classification, IWSLT’14 DE-EN/WMT’16 EN-DE for neural machine translation, and the GLUE benchmark for natural language understanding. The implementations are based on PyTorch, and we run the experiments on Nvidia V100 GPUs. In both the image and language tasks, after tuning the weight decay carefully, we find the decoupled weight decay [15] gives much better results for ADAM, MADAM, LAPROP and LAMADAM. Therefore, we use this approach in all of our experiments. Across the plots in this section, we define the average step size at time t as the average of $|\eta_t m_t / (\sqrt{v_t} + \epsilon)|$ for ADAM/MADAM and $|\eta_t m_t|$ for LAPROP/LAMADAM over all the entries.

5.1 Image Classification

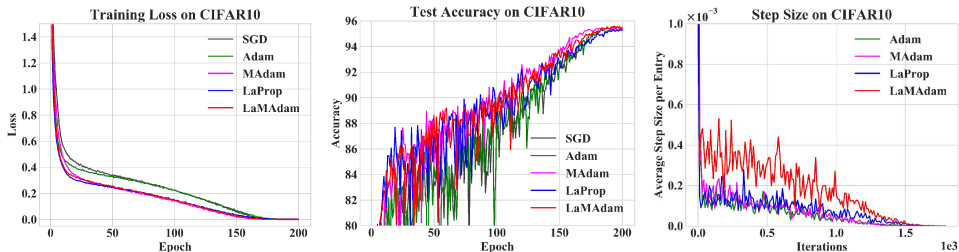


Figure 3: Training loss, test accuracy and average step size on CIFAR10.

To evaluate the effectiveness of MVA for image classification, we compare with SGD, ADAM and LAPROP in training ResNet18 [9] on CIFAR10, CIFAR100 and ImageNet. On all datasets, we perform a grid search for the learning rate and weight decay and report the best results for each method in Table 1. For CIFAR10/100, we adopt the ResNet18 from a public repository.² We use a batch size of 128 and train the model for 200 epochs. Instead of using the multistep schedule, we find the cosine learning rate schedule to give better results for both SGD and adaptive methods. Therefore, we set a final learning rate of $2e-6$ in all cases. We also find AMSGrad [21] to improve the classification accuracy of all adaptive methods evaluated on CIFAR10/100, and we apply AMSGrad in all experiments with adaptive methods. Further details are in Appendix D. On ImageNet, we use the implementation from torchvision and the default learning rate schedule, multiplying the learning rate by 0.1 every 30 epochs and train a total of 90 epochs, with a batch size of 256. We do not use AMSGrad in this case.

Despite we achieved a marginal improvement on CIFAR10, adaptive methods often cannot beat carefully tuned SGD on CIFAR100 and ImageNet when training popular architectures such as ResNet, as confirmed by results such as [28, 35, 13]. Nevertheless, with the proposed MVA, we shrink the gap between adaptive methods and carefully tuned SGD for training convolutional networks on these image classification datasets, and achieved a top-1 accuracy very close to SGD on ImageNet.

5.2 Neural Machine Translation

We train Transformers [26] from scratch with LAPROP and LAMADAM on IWSLT’14 German-to-English (DE-EN) translation dataset [3] and WMT’16 English-to-German (EN-DE) translation

Model	CIFAR-10	CIFAR-100	ImageNet
SGD	95.44 (.04)	79.62 (.07)	70.18
ADAM	95.37 (.03)	78.77 (.07)	66.54
LAPROP	95.34 (.03)	78.36 (.07)	70.02
MADAM	95.51 (.09)	79.32 (.08)	69.96
LAMADAM	95.38 (.11)	79.21 (.11)	70.16

Table 1: Accuracies on CIFAR10/100 and ImageNet. The ADAM results on ImageNet is copied from [13]. CIFAR10/100 experiments are the median (standard error) over 4 runs.

²<https://github.com/kuangliu/pytorch-cifar>

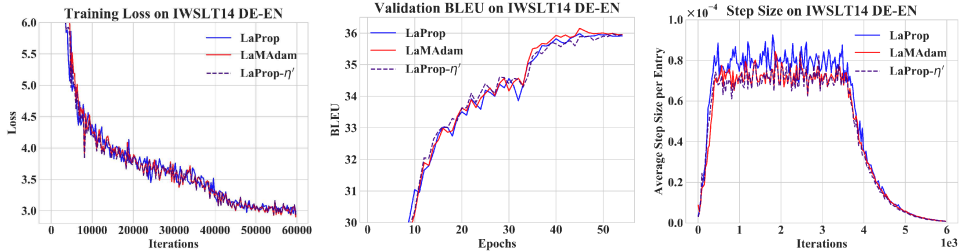


Figure 4: Training loss, validation BLEU and average step size on IWSLT’14 DE-EN, trained with $\eta=5e-4$, $\lambda=1e-2$, $\beta=0.999$ for LAPROP and $\eta=1.5e-3$, $\lambda=1e-2$, $\underline{\beta}=0.5$, $\beta=0.999$ for LAMADAM, and $\eta=4.375e-4$, $\lambda=1e-2$, $\beta=0.999$ for LAPROP- η' .

dataset, based on the implementation of fairseq.³ We do not compare with SGD, since it is unstable for Transformers [34]. IWSLT’14 DE-EN has 160k training examples, while WMT’16 EN-DE has 4.5M training examples.

For IWSLT’14 DE-EN, we use 512-dimensional word embeddings and 6 Transformer blocks with 4 attention heads and 1024 FFN dimensions for the encoder/decoder. To demonstrate the full potential of adaptive methods under constant learning rates, we use the tristage learning rate schedule [19], linearly increase the learning rate from 0.01η to the full learning rate η in 4k iterations, hold it at η for 32k iterations, and exponentially decay it to 0.01η in 24k iterations. We train a total of 60k iterations, during which each minibatch has up to 4096 tokens. Results are summarized in Table 2, where the baseline’s BLEU score is already 1.22 higher than the best results reported in [13] using the same model. Figure 4 shows the training dynamics of LAPROP and LAMADAM. Despite using 3 times higher learning rate, the average update size of LAMADAM is smaller, but LAMADAM shows slightly better convergence on the training set and better validation BLEU. This may be explained by the heavy-tailed distribution of the gradient in the process of training transformers from scratch [34], and smaller step sizes mitigating the effect of extreme gradient values on the model’s performance. It is worth mentioning that LAPROP diverges using the large learning rate $1.5e-3$.

Further, we find LAPROP produces a similar step size curve as LAMADAM with learning rate $4.375e-4$, but with weaker performance than LAMADAM. LAMADAM uses the maximum variation rule to select the adaptive learning rate for each dimension, creating benefit that is not achievable by simply scaling the base learning rate η .

Method	IWSLT’14 DE-EN	WMT’16 EN-DE
LAPROP	35.98 (0.06)	27.02
LAMADAM	36.09 (0.04)	27.11

Table 2: BLEU score of LAPROP and LAMADAM for training transformers on machine translation datasets. We report the median and standard error for IWSLT’14 over 5 runs.

For WMT’16, we aim to evaluate our approaches on large-scale datasets/models like in [18], and use 1024-dimensional word embeddings, 6 transformer blocks with 16 attention heads and 4096 FFN dimensions for the encoder/decoder. Each minibatch has up to 480k tokens and we train for 32k iterations, and use the inverse square root learning rate schedule with 4k step warmup [26]. We evaluate the *single model* BLEU on newstest2013, unlike [13] where models from the last 20 epochs are averaged to get the results. As shown in Table 2, LAMADAM also achieves better results. Further implementation details are provided in Appendix E

5.3 General Language Understanding Evaluation (GLUE)

To evaluate the efficacy of MVA for transfer learning, we finetune pre-trained language models on the GLEU benchmark [27]. GLUE is a collection of 9 natural language understanding tasks, formulated into classification and regression problems. Following prevalent validation settings [5, 12, 20], we report the median and standard error for finetuning the RoBERTa-base model [14] over 4 runs with the same hyperparameters but different random seeds on the dev set of 8 of the 9 tasks, and report the results in Table 3. MADAM and LAMADAM give better scores than the corresponding baselines in the 8 tasks. More experimental details are given in Appendix F.

³<https://github.com/pytorch/fairseq>.

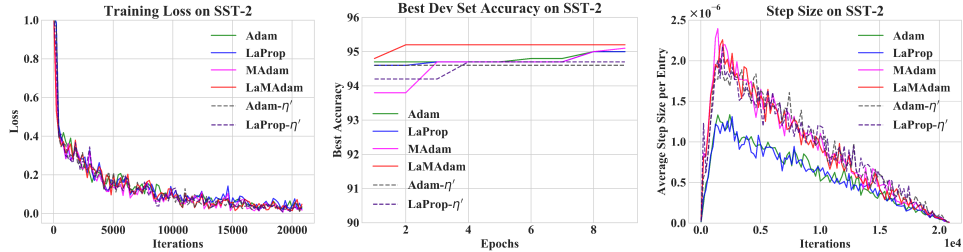


Figure 5: Training loss, validation accuracy and step size of various optimization methods on SST-2. All optimizers here use $\lambda = 0.1$. ADAM and LAPROP use $(\eta, \beta)=(1e-5, 0.98)$, MADAM and LAMADAM use $(\eta, \underline{\beta}, \bar{\beta})=(4e-5, 0.5, 0.98)$, ADAM- η' and LAPROP- η' use $(\eta, \beta)=(1.6e-5, 0.98)$.

Method	MNLI (Acc)	QNLI (Acc)	QQP (Acc)	RTE (Acc)	SST-2 (Acc)	MRPC (Acc)	CoLA (Mcc)	STS-B (Pearson)
Reported [14]	87.6	92.8	91.9	78.7	94.8	90.2	63.6	91.2
ADAM	87.70 (.03)	92.85 (.06)	91.80 (.03)	79.25 (.71)	94.75 (.08)	88.50 (.24)	61.92 (1.1)	91.17 (.13)
LAPROP	87.80 (.04)	92.85 (.13)	91.80 (.03)	78.00 (.46)	94.65 (.11)	89.20 (.20)	63.01 (.61)	91.17 (.06)
MADAM	87.90 (.08)	92.95 (.07)	91.85 (.03)	79.60 (.66)	94.85 (.12)	89.70 (.17)	63.33 (.60)	91.28 (.03)
LAMADAM	87.80 (.03)	93.05 (.05)	91.85 (.05)	80.15 (.64)	95.15 (.15)	90.20 (.20)	63.84 (.85)	91.36 (.04)

Table 3: Results (median and variance) on the dev sets of GLUE based on finetuning the RoBERTa-base model, from 4 runs with the same hyperparameter but different random seeds.

To highlight the difference of the optimizers on transfer learning, we compare the training loss, dev set accuracy and the average step size on SST-2, as shown in Figure 5. Different from Machine Translation experiments where we train the Transformers from scratch, the adaptive step size of MADAM/LAMADAM is higher.⁴ Because we start from a pre-trained model, the heavy tail of the gradient is alleviated, just as the BERT model in the later stage of training as shown in [34], but still MVA helps in this situation. Same as in Machine Translation experiments, the highest test accuracy of ADAM/LAPROP cannot reach the same value as MADAM/LAMADAM by simply scaling the base learning rate η to reach similar step sizes as MADAM/LAMADAM.

6 Related Work

Our work is motivated by recent advances in optimizing deep neural networks, particularly Transformers, on adaptive learning rates and heuristic warmup.

Adaptive Learning Rate Many studies have focused on achieving more reliable convergence with adaptive step sizes [11, 6, 25, 32]. [21] proposed to compute the adaptive learning rate with the coordinate-wise maximum value of the running squared gradient. ADABOUND [16] clips the adaptive learning rate of ADAM with a decreasing upper bound and an increasing lower bound. Lookahead [35] computes weight updates by looking ahead at the sequence of “fast weights” generated by another optimizer. LAPROP [37] uses local running estimation of the variance to normalize the gradients, resulting in higher empirical stability. [30] proposed Layer-wise Adaptive Rate Scaling (LARS), and scaled the batch size to 16,384 for training ResNet50. LAMB [31] is proposed to improve LARS on training BERT. Different from these methods, we focus on finding the adaptive averaging coefficients.

Learning Rate Warmup It is observed that adaptive learning schemes may lead to bad local optima and must be adjusted through linear learning rate scaling and warmup heuristics [8, 7]. Similar phenomena are observed in other natural language processing tasks [2, 26]. Most theoretical analysis about linear learning rate scaling considers stochastic gradient descent only [10, 23]. Our approach uses an aggressive averaging coefficient and smaller learning rate for abnormal gradients, which stabilize the training adaptively.

⁴MADAM/LAMADAM use $4x \eta$ than ADAM/LAPROP and the step size is about 1.8x on GLEU, while on IWSLT’14 the two ratios are 2 and (approximately) 0.875.

7 Conclusion

In this paper, we present Maximum Variation Averaging (MVA), a novel adaptive learning rate scheme that replaces the exponential running average of squared gradient with an adaptive weighted mean. In each step, MVA chooses the weight β_t for each coordinate, such that the estimated gradient variance is maximized. This enables MVA to take smaller steps when large curvatures or abnormal gradients are present, which leads to more desirable convergence behaviors in face of gradient noise. We illustrate how our proposed models improve convergence by a better adaptation to variance and demonstrate strong empirical results on a wide range of tasks including image classification, neural machine translation and natural language understanding.

8 Broader Impacts

Transformer models are quickly becoming a central tool for analyzing text, and have the potential to make web content better moderated, more accessible to readers that speak under-resourced languages, are more available to readers with visual impairments. Unfortunately, the development of Transformer models is slowed by the difficulty and expense of optimizing this relatively new class of models, and their reliance of adaptive optimizers that are not well-understood. As a result, research in this area is largely conducted by large companies with huge computing resources for tuning optimization parameters.

Our goal with this work is to take a step towards making adaptive optimizers more reliable, faster, and easy to use. While research in this direction is fairly technical, it has the broader potential to contribute to a better internet with better translation and moderation tools. It also has the potential to help democratize language modelling, making it more accessible to organizations with modest computing budgets.

References

- [1] Lukas Balles and Philipp Hennig. Dissecting adam: The sign, magnitude and variance of stochastic gradients. In *ICML*, pages 404–413, 2018.
- [2] Nikolay Bogoychev, Kenneth Heafield, Alham Fikri Aji, and Marcin Junczys-Dowmunt. Accelerating asynchronous stochastic gradient descent for neural machine translation. In *EMNLP*, 2018.
- [3] Mauro Cettolo, Jan Niehues, Sebastian Stüker, Luisa Bentivogli, and Marcello Federico. Report on the 11th iwslt evaluation campaign, iwslt 2014. In *Proceedings of the International Workshop on Spoken Language Translation, Hanoi, Vietnam*, volume 57, 2014.
- [4] Xiangyi Chen, Sijia Liu, Ruoyu Sun, and Mingyi Hong. On the convergence of a class of adam-type algorithms for non-convex optimization. *ICLR*, 2019.
- [5] Jacob Devlin, Ming-Wei Chang, Kenton Lee, and Kristina Toutanova. Bert: Pre-training of deep bidirectional transformers for language understanding. In *NAACL*, pages 4171–4186, 2019.
- [6] John Duchi, Elad Hazan, and Yoram Singer. Adaptive subgradient methods for online learning and stochastic optimization. *Journal of Machine Learning Research*, pages 2121–2159, 2011.
- [7] Akhilesh Gotmare, Nitish Shirish Keskar, Caiming Xiong, and Richard Socher. A closer look at deep learning heuristics: Learning rate restarts, warmup and distillation. In *ICLR*, 2019.
- [8] Priya Goyal, Piotr Dollár, Ross Girshick, Pieter Noordhuis, Lukasz Wesolowski, Aapo Kyrola, Andrew Tulloch, Yangqing Jia, and Kaiming He. Accurate, large minibatch sgd: Training imagenet in 1 hour. *arXiv:1706.02677*, 2017.
- [9] Kaiming He, Xiangyu Zhang, Shaoqing Ren, and Jian Sun. Deep residual learning for image recognition. In *CVPR*, pages 770–778, 2016.
- [10] Elad Hoffer, Itay Hubara, and Daniel Soudry. Train longer, generalize better: closing the generalization gap in large batch training of neural networks. In *Neurips*, pages 1731–1741. 2017.
- [11] Diederik P. Kingma and Jimmy Ba. Adam: A method for stochastic optimization. In Yoshua Bengio and Yann LeCun, editors, *ICLR*, 2015.
- [12] Zhenzhong Lan, Mingda Chen, Sebastian Goodman, Kevin Gimpel, Piyush Sharma, and Radu Soricut. Albert: A lite bert for self-supervised learning of language representations. *ICLR*, 2020.
- [13] Liyuan Liu, Haoming Jiang, Pengcheng He, Weizhu Chen, Xiaodong Liu, Jianfeng Gao, and Jiawei Han. On the variance of the adaptive learning rate and beyond. *ICLR*, 2020.

- [14] Yinhan Liu, Myle Ott, Naman Goyal, Jingfei Du, Mandar Joshi, Danqi Chen, Omer Levy, Mike Lewis, Luke Zettlemoyer, and Veselin Stoyanov. Roberta: A robustly optimized bert pretraining approach. *arXiv:1907.11692*, 2019.
- [15] Ilya Loshchilov and Frank Hutter. Fixing weight decay regularization in adam. 2018.
- [16] Liangchen Luo, Yuanhao Xiong, Yan Liu, and Xu Sun. Adaptive gradient methods with dynamic bound of learning rate. *ICLR*, 2019.
- [17] Jerry Ma and Denis Yarats. On the adequacy of untuned warmup for adaptive optimization. *arXiv:1910.04209*, 2019.
- [18] Myle Ott, Sergey Edunov, David Grangier, and Michael Auli. Scaling neural machine translation. In *Proceedings of the Third Conference on Machine Translation*, pages 1–9, 2018.
- [19] Daniel S Park, William Chan, Yu Zhang, Chung-Cheng Chiu, Barret Zoph, Ekin D Cubuk, and Quoc V Le. SpecAugment: A simple data augmentation method for automatic speech recognition. *Interspeech*, pages 2613–2617, 2019.
- [20] Colin Raffel, Noam Shazeer, Adam Roberts, Katherine Lee, Sharan Narang, Michael Matena, Yanqi Zhou, Wei Li, and Peter J Liu. Exploring the limits of transfer learning with a unified text-to-text transformer. *arXiv:1910.10683*, 2019.
- [21] Sashank J Reddi, Satyen Kale, and Sanjiv Kumar. On the convergence of adam and beyond. *ICLR*, 2018.
- [22] Tom Schaul, Sixin Zhang, and Yann LeCun. No more pesky learning rates. In *ICML*, pages 343–351, 2013.
- [23] Samuel L. Smith, Pieter-Jan Kindermans, and Quoc V. Le. Don’t decay the learning rate, increase the batch size. In *ICLR*, 2018.
- [24] Nitish Srivastava, Geoffrey Hinton, Alex Krizhevsky, Ilya Sutskever, and Ruslan Salakhutdinov. Dropout: a simple way to prevent neural networks from overfitting. *The journal of machine learning research*, 15(1):1929–1958, 2014.
- [25] T. Tieleman and G. Hinton. Lecture 6.5—RmsProp: Divide the gradient by a running average of its recent magnitude. COURSERA: Neural Networks for Machine Learning, 2012.
- [26] Ashish Vaswani, Noam Shazeer, Niki Parmar, Jakob Uszkoreit, Llion Jones, Aidan N. Gomez, Lukasz Kaiser, and Illia Polosukhin. Attention is all you need. In *NeurIPS*, 2017.
- [27] Alex Wang, Amanpreet Singh, Julian Michael, Felix Hill, Omer Levy, and Samuel R Bowman. Glue: A multi-task benchmark and analysis platform for natural language understanding. *EMNLP*, page 353, 2018.
- [28] Ashia C Wilson, Rebecca Roelofs, Mitchell Stern, Nati Srebro, and Benjamin Recht. The marginal value of adaptive gradient methods in machine learning. In *Neurips*, pages 4148–4158, 2017.
- [29] Yuhuai Wu, Mengye Ren, Renjie Liao, and Roger Grosse. Understanding short-horizon bias in stochastic meta-optimization. *arXiv:1803.02021*, 2018.
- [30] Yang You, Igor Gitman, and Boris Ginsburg. Scaling SGD batch size to 32k for imagenet training. *CoRR*, abs/1708.03888, 2017.
- [31] Yang You, Jing Li, Sashank Reddi, Jonathan Hseu, Sanjiv Kumar, Srinadh Bhojanapalli, Xiaodan Song, James Demmel, Kurt Keutzer, and Cho-Jui Hsieh. Large batch optimization for deep learning: Training bert in 76 minutes. In *International Conference on Learning Representations*, 2020.
- [32] Matthew D. Zeiler. ADADELTA: an adaptive learning rate method. *CoRR*, abs/1212.5701, 2012.
- [33] Guodong Zhang, Lala Li, Zachary Nado, James Martens, Sushant Sachdeva, George Dahl, Chris Shallue, and Roger B Grosse. Which algorithmic choices matter at which batch sizes? insights from a noisy quadratic model. In *NeurIPS*, pages 8194–8205, 2019.
- [34] Jingzhao Zhang, Sai Praneeth Karimireddy, Andreas Veit, Seungyeon Kim, Sashank J Reddi, Sanjiv Kumar, and Suvrit Sra. Why adam beats sgd for attention models. *arXiv:1912.03194*, 2019.
- [35] Michael R. Zhang, James Lucas, Jimmy Ba, and Geoffrey E. Hinton. Lookahead optimizer: k steps forward, 1 step back. In *NeurIPS*, pages 9593–9604, 2019.
- [36] Chen Zhu, Yu Cheng, Zhe Gan, Siqi Sun, Tom Goldstein, and Jingjing Liu. FreeLB: Enhanced adversarial training for natural language understanding. In *ICLR*, 2020.
- [37] Liu Ziyin, Zhikang T Wang, and Masahito Ueda. Laprop: a better way to combine momentum with adaptive gradient. *arXiv:2002.04839*, 2020.

Adaptive Learning Rates with Maximum Variation Averaging (Appendix)

A Deriving the closed form solution Eq.8

Plugging Eq. 4,5,6, and the unbiased estimations $u_t(\beta) = \tilde{u}_t(\beta)/w_t(\beta)$, $v_t(\beta) = \tilde{v}_t(\beta)/w_t(\beta)$ into Eq. 7, each coordinate is solving the same problem:

$$\arg \max_{\beta} f(\beta) = \frac{\beta w_{t-1} v_{t-1} + (1-\beta) g_t^2}{\beta w_{t-1} + (1-\beta)} - \left[\frac{\beta w_{t-1} u_{t-1} + (1-\beta) g_t}{\beta w_{t-1} + (1-\beta)} \right]^2. \quad (14)$$

Let $\gamma = 1/[\beta w_{t-1} + (1-\beta)] \in [1, 1/w_{t-1}]$, we can see $f(\beta)$ can be represented as a quadratic function of γ . Specifically,

$$f(\beta) = h(\gamma) = \frac{w_{t-1} v_{t-1} - g_t^2}{w_{t-1} - 1} + \left[g_t^2 - \frac{w_{t-1} v_{t-1} - g_t^2}{w_{t-1} - 1} \right] \gamma - \left\{ \frac{w_{t-1} u_{t-1} - g_t}{w_{t-1} - 1} + \left[g_t - \frac{w_{t-1} u_{t-1} - g_t}{w_{t-1} - 1} \right] \gamma \right\}^2.$$

Meanwhile, β is a monotonic function of γ . Therefore, $f(\beta)$ has a unique maximum value.

To find the maximum value, we return to Eq. 14, from which we can find a stationary point

$$\frac{v_{t-1} - u_{t-1}^2 + (g_t - u_{t-1})^2}{w_{t-1} [(g_t - u_{t-1})^2 - v_{t-1} + u_{t-1}^2] + v_{t-1} - u_{t-1}^2 + (g_t - u_{t-1})^2}. \quad (15)$$

B Practical notes of β_t

Claims and arguments:

1. For $t > 1$, since $0 < \beta_t \leq 1$, w_t will monotonically increase from $(1 - \beta_1)$ to 1.

This is obvious since in every step, w_t is an interpolation between w_{t-1} and 1, and $w_t \geq w_{t-1}$. We have also set $w_1 = 1 - \beta_1$.

2. For any g_t, u_{t-1}, v_{t-1} satisfying $v_{t-1} - u_{t-1}^2 > 0$ in Eq. 8, we have $\beta_t \in [1/(1 + w_{t-1}), 1/(1 - w_{t-1})]$.

Eq. 10 is monotonic in R_t . Since g_t can be any value, R_t can be any value from 0 to ∞ . If $R_t = 0$, β_t takes the largest value $1/(1 - w_t)$. If $R_t \rightarrow \infty$, $\beta_t \rightarrow 1/(w_t + 1)$.

3. As $t \rightarrow \infty$, $w_t \rightarrow 1$ and $\beta_t \in [0.5, \infty]$.

Combining Claims 1 and 2 to get this result.

4. Adding a small coefficient $\delta > 0$ to the denominator of Eq. 8 has negligible effect on the value of β_t and does not violate the maximum variation objective (Eq. 7).

Since δ is small, it has negligible effect on β_t when division by zero does not happen. We only need to confirm adding δ will not affect the solution when division by zero happens. We can re-write the dividend of Eq. 8 as

$$(w_{t-1} + 1)(g_t - u_{t-1})^2 + (1 - w_{t-1})(v_{t-1} - u_{t-1}^2). \quad (16)$$

Since $\mathbb{E}[X^2] - (\mathbb{E}[X])^2 = \text{Var}[X] \geq 0$, we can conclude that $v_{t-1} - u_{t-1}^2 \geq 0$.

When $1 - \beta_1 \leq w_{t-1} < 1$, Eq. 16 can be 0 only when $g_t = u_{t-1}$ and $v_{t-1} = u_{t-1}^2$. In this special case, we can set β_t to any value in $[0, 1]$ without changing $\tilde{\sigma}_t^2$; we will always have $v_t = \tilde{v}_{t-1}/w_{t-1} = v_{t-1}$, $u_t = \tilde{u}_{t-1}/w_{t-1} = u_{t-1}$, and $\tilde{\sigma}_t^2 = 0$. Only $w_t = (w_{t-1} - 1)\beta_t + 1$ is affected by β_t , which takes a larger value when β_t is smaller. The solution given by adding δ to the denominator is $\beta_t = 0$, and the following clipping will set $\beta_t = \underline{\beta}$, resulting in the largest possible $w_t = (w_{t-1} - 1)\underline{\beta} + 1$. In the next step, if Eq. 16 is not zero, then we have $\beta_{t+1} = 1/(w_t + 1)$, and we know $g_{t+1} \neq u_t$.⁵ In this case, for $0.5 \leq \beta_{t+1} < 1$, $\tilde{\sigma}_{t+1}^2$ increases as β_{t+1} decreases, so setting w_t to its maximum will achieve the maximum variance at the next step. Otherwise if Eq. 16 is zero, doing this will not change $\tilde{\sigma}_{t+1}^2 = 0$.

When $w_{t-1} = 1$, Eq. 16 is 0 if and only if $g_t = u_{t-1}$. As a result, if $v_{t-1} = u_{t-1}^2$, we have the same conclusion as before. Otherwise, $\beta_t = (v_{t-1} - u_{t-1}^2)/\delta$ before clipping, and $\beta_t = \bar{\beta}$ after clipping. Also, any $0 < \beta_t < 1$ will not change the value of $u_t = \beta_t u_{t-1} + (1 - \beta_t) g_t = u_{t-1}$. Since $g_t^2 = u_{t-1}^2 < v_{t-1}$, to maximize $\tilde{\sigma}_t^2 = v_t(\beta) - u_{t-1}^2$, we should set $\beta_t = \bar{\beta}$ so that $v_t(\beta)$ takes the maximum value, which is consistent with the solution after adding δ to the denominator.

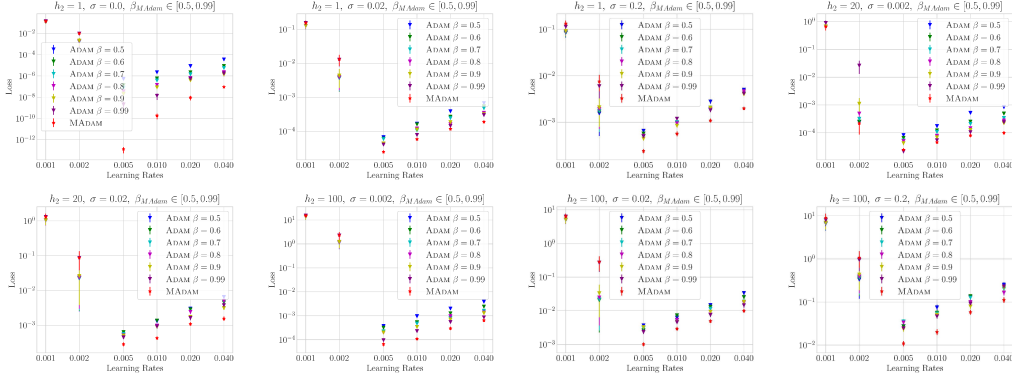


Figure 6: More results on the Noisy Quadratic Model.

C Additional Experimental Results on the Noisy Quadratic Model

In this section, we give more results comparing ADAM and MADAM on the Noisy Quadratic Model. The results are shown in Figure 6. Generally, the best result of MADAM has a more significant margin when h_2 and σ are higher, i.e., the improvement is more significant when the problem is worse conditioned and the noise level is higher. Note that for each trial, we start both algorithms from the same random initialization.

D Additional Details of Experiments on Image Classification

For ADAM and LAPROP, we set $\beta = 0.999$. For MADAM and LAMADAM, we set $\underline{\beta} = 0.5$ and $\bar{\beta} = 0.999$ in all cases. On CIFAR10 and CIFAR100, we use random cropping (4-pixel zero paddings on each side) and random horizontal flip as the data augmentations. On ImageNet, we use random resized crop and random horizontal flip for data augmentation. For each optimizer, we do a grid search over the learning rate and weight decay for the best hyperparameters.

Hyperparameters of CIFAR10. Except for SGD, we tried learning rates from $\{5e-4, 1e-3, 2e-3, 3e-3, 4e-3, 6e-3, 8e-3\}$ and weight decay from $\{0.025, 0.05, 0.1, 0.2, 0.4, 0.8, 1\}$. The best learning rate and weight decay for ADAM, LAPROP, MADAM and LAMADAM are $(3e-3, 0.2)$, $(1e-3, 0.4)$, $(8e-3, 0.05)$ and $(6e-3, 0.05)$ respectively. As to SGD, we tried learning rates from $\{3e-2, 5e-2, 1e-1, 2e-1, 3e-1\}$ and weight decays from $\{1e-4, 3e-4, 5e-4, 1e-3, 2e-3\}$, and the best result was achieved with learning rate $2e-1$ and weight decay $3e-4$. These hyperparameters that gave the best results are also the hyperparameters we used for plotting Figure 3.

Hyperparameters for CIFAR100. We use the same grid search configurations as for CIFAR10. The best learning rate and weight decay for ADAM, LAPROP, MADAM and LAMADAM are $(2e-3, 0.4)$, $(5e-4, 1)$, $(4e-3, 0.2)$ and $(3e-3, 0.2)$ respectively. For SGD, the best learning rate and weight decay are $3e-2$ and $2e-3$ respectively.

Hyperparameters for ImageNet. Due to the heavy workload and the time limit, we were not able to accomplish 4 runs for each hyperparameter in ImageNet, so we report the best results for each optimizer in Table 5.1, except for the result of ADAM, which was copied from [13] but uses the same hyperparameters except for the learning rate and weight decay. For LAPROP, MADAM and LAMADAM, we choose learning rates from $\{1e-3, 2e-3, 3e-3, 4e-3, 5e-3, 6e-3, 8e-3\}$ and weight decay from $\{0.003, 0.006, 0.01, 0.012, 0.02, 0.03\}$, and found the best combinations for LAPROP, MADAM and LAMADAM are $(2e-3, 0.03)$, $(5e-3, 0.012)$ and $(6e-3, 0.012)$. For SGD, we choose learning rate from $\{0.05, 0.1, 0.2\}$ and weight decay from $\{5e-5, 7e-5, 1e-4\}$, and found the best combination to be $(0.1, 7e-5)$.

E Additional Details of Experiments on the Machine Translation

For LAPROP, we tried β from $\{0.98, 0.99, 0.997, 0.999\}$. We found 0.999 to work the best and used it for all the grid search experiments. For LAMADAM, we set $\beta = 0.5$, $\bar{\beta} = 0.999$. We use `transformer_iwslt_de_en` and `transformer_vaswani_wmt_en_de_big` architectures defined in fairseq for IWSLT'14 and WMT'16, respectively.

⁵Otherwise we will still have $g_{t+1} = u_t$, $g_{t+1}^2 = u_t^2 = v_t$ and Eq. 16 is 0.

Hyperparameters for IWSLT’14. We do a grid search for the learning rate and weight decay for both optimizers. We tried η from $\{2.5e-4, 5e-4, 1e-3, 1.5e-3, 2e-3\}$, and weight decay from $\{0.0001, 0.001, 0.01, 0.1\}$. The best combinations for LAPROP and LAMADAM are $(5e-4, 0.01)$ and $(1.5e-3, 0.01)$. For other hyperparameters, we use the default setting in the fairseq example, which sets dropout probability to 0.3, uses label smoothed cross entropy loss with a smoothing coefficient 0.1, and shares the input and output token embedding parameters.

Hyperparameters for WMT’16. The default implementation from fairseq did not use weight decay, so we also ignore weight decay in all experiments. For LAPROP, we found $\beta = 0.98$ to give the best results, and we set $\underline{\beta} = 0.95, \bar{\beta} = 0.98$ in all experiments. This takes around 8 hours on 16 V100 GPUs each run. For grid search, we tried η from $\{5e-4, 1e-3, 1.5e-3, 2e-3\}$, and found $1e-3$ and $1.5e-3$ to work the best for LAPROP and LAMADAM respectively. Other hyperparameters are the defaults of the corresponding fairseq example, which uses a dropout probability of 0.3, the label smoothed cross entropy loss with a smoothing coefficient 0.1, and shares all embedding parameters.

F Additional Details of Experiments on the GLUE benchmark

It is reported in [14] that ADAM is sensitive to the choice of ϵ on GLUE. Following their settings, we set $\epsilon = 1e-6$ for both ADAM and MADAM. For LAPROP and LAMADAM, however, we always set $\epsilon = 1e-15$, like all other experiments in this paper, which is consistent with the observation in [37] that LAPROP is robust to the choice of ϵ . We set $\beta = 0.98$ for ADAM and LAPROP, and $\underline{\beta} = 0.5, \bar{\beta} = 0.98$ for LAPROP and LAMADAM. All other hyperparameters are set to the same as the example in fairseq.⁶ For each task, we do a grid search over the learning rate and weight decay, which are chosen from $\{5e-6, 1e-5, 2e-5, 4e-5, 5e-5, 6e-5\}$ and $\{0.025, 0.05, 0.1, 0.2\}$ respectively. We list the best combinations for ADAM, MADAM, LAPROP and LAMADAM on each task as below:

MNLI: $(1e-5, 0.1), (1e-5, 0.1), (4e-5, 0.025), (4e-5, 0.025)$.

QQP: $(1e-5, 0.1), (1e-5, 0.1), (4e-5, 0.025), (4e-5, 0.025)$.

QNLI: $(1e-5, 0.1), (1e-5, 0.1), (4e-5, 0.05), (4e-5, 0.05)$.

SST-2: $(1e-5, 0.1), (1e-5, 0.1), (4e-5, 0.1), (4e-5, 0.1)$.

RTE: $(2e-5, 0.1), (2e-5, 0.1), (6e-5, 0.1), (6e-5, 0.1)$.

MRPC: $(1e-5, 0.1), (1e-5, 0.1), (6e-5, 0.1), (6e-5, 0.1)$.

STS-B: $(2e-5, 0.1), (2e-5, 0.1), (4e-5, 0.5), (4e-5, 0.5)$.

CoLA: $(2e-5, 0.1), (2e-5, 0.1), (6e-5, 0.5), (6e-5, 0.5)$.

⁶<https://github.com/pytorch/fairseq/blob/master/examples/roberta/README.glue.md>